

Article

A Comparative Study on the Effect of Peri-Implant Infection Management Lasers (1064-nm Q-Switch Nd:YAG, 1064-nm Nd:YAG and 980-nm Diode) on Titanium Grade 4 Surface

Claudio Pasquale ^{1,2,*}, Nicola De Angelis ^{1,2}, Elena Dellacasa ³, Roberto Raiteri ³, Fabrizio Barberis ², Alberto Lagazzo ², Stefano Benedicenti ¹ and Andrea Amaroli ^{4,*}

¹ Department of Surgical and Diagnostic Sciences, University of Genoa, 16132 Genoa, Italy

² Department of Civil, Chemical and Environmental Engineering, University of Genoa, 16100 Genoa, Italy

³ Dipartimento di Informatica, Bioingegneria, Robotica e Ingegneria dei Sistemi, University of Genoa, 16132 Genoa, Italy

⁴ Department of Orthopedic Dentistry, Faculty of Dentistry, First Moscow State Medical University (Sechenov University), 119991 Moscow, Russia

* Correspondence: clodent@gmail.com (C.P.); andrea.amaroli@unige.it (A.A.)

Featured Application: This study provides information about the effects of laser irradiation provided against peri-implant infection on titanium and supports the best choice of having lesser titanium implant damage.

Abstract: Over the past 10 years, the number of dental implants has grown significantly. This increase has consequently led to an elevation of the statistics related to cases of peri-implantitis. Laser therapy has conquered a place among the therapies of excellence to treat peri-implantitis. However, the laser device used could influence the therapy's success. The aim of this comparative experimental work was to highlight the differences in the work on grade 4 titanium surfaces of the most commonly used laser lights in this field, taking into consideration any structural damage that lasers could cause to implant surfaces. The lasers examined were a 980 nm diode laser; a 1064 nm Nd:YAG laser; and a new generation of 1064 nm Nd:YAG Q-switch nano pulsed laser. We evaluated the titanium temperature increase, the pre- and post-treatment two-dimensional surface appearance observed under the scanning electron microscope; finally, the three-dimensional pre- and post-treatment topographic analysis was assessed using atomic force microscopy. We showed that the 1064-nm Q-switch Nd:YAG nanosecond pulsed laser appears to be more suitable for the preservation of implant morphology because of the absence of the induction of metal damage.

Keywords: peri-implantitis; titanium surfaces; biofilm; decontamination; implant



Citation: Pasquale, C.; De Angelis, N.; Dellacasa, E.; Raiteri, R.; Barberis, F.; Lagazzo, A.; Benedicenti, S.; Amaroli, A. A Comparative Study on the Effect of Peri-Implant Infection Management Lasers (1064-nm Q-switch Nd:YAG, 1064-nm Nd:YAG and 980-nm Diode) on Titanium Grade 4 Surface. *Appl. Sci.* **2023**, *13*, 125. <https://doi.org/10.3390/app13010125>

Academic Editors: Morena Petrini and Stefano Gennai

Received: 9 November 2022

Revised: 16 December 2022

Accepted: 20 December 2022

Published: 22 December 2022



Copyright: © 2022 by the authors. Licensee MDPI, Basel, Switzerland. This article is an open access article distributed under the terms and conditions of the Creative Commons Attribution (CC BY) license (<https://creativecommons.org/licenses/by/4.0/>).

1. Introduction

Implant-supported prosthesis is considered one of the finest and most common approaches used to replace missing teeth [1]. About 12 million dental implants are placed every year worldwide [2]. However, a significant increase in peri-implant diseases was recently described. Similar to periodontal diseases, the main cause of peri-implant diseases is dental plaques, which supports correlated pathogenic bacterial growth [3]. Indeed, periodontal health is influenced by various factors such as oral hygiene, genetic and epigenetic factors, systemic health, and nutrition [4,5]. The recent literature shows that the prevalence of peri-implantitis is equal to 10% of the implants and 20% of the patients, while peri-implant mucositis affects about 30% of the sites and 50% of the subjects treated [2]. However, despite many preventive treatment approaches being suggested, nowadays, it is not possible to identify a reliable and consistent therapy for the treatment of these pathologies [6]; the prevention and sudden management of early symptomatology appear

to be the most effective protocol [7,8]. Indeed, it is known that the incidence of peri-implant diseases can be minimised through routine dental biofilm control. Recently, laser therapies have gained acceptance for the management of peri-implant mucositis [6].

Systematic reviews point out the wide range of wavelengths, powers, energies, time, and number of applications suggested for peri-implant disease treatments, leading to the conclusion of a non-univocal approach [9–12]. However, semiconductor lasers such as diodes and solid-state lasers, including 1064-nm Neodymium-Doped Yttrium Aluminum Garnet (Nd:YAG) and Erbium:YAG, seem to better support laser therapy advances [13]. Indeed, according to the wavelengths employed and the therapy parameters administered, several laser features through photodynamic therapies and photobiomodulation as well as surgery can be exploited. Therefore, diseased tissue may be removed [7,8], inflammation reduced [11], and wound healing improved [14]; pathogenic bacteria can be killed or inhibited, and natural microbiota can be stimulated [15]. In particular, the evidence-based literature shows that laser therapies can decontaminate the implant surface and surrounding areas [6] and stimulate disease-impacted tissue recovery [9,16,17].

However, the incomplete knowledge of interactions between the peri-implant titanium with laser wavelengths and clinical parameters limits the laser application in peri-implantitis management [18]. The authors suggested that lasers can damage titanium screws because of temperature and trigger tissue necrosis [19] and microbiota biofilm alterations [20]. Therefore, despite the effective support of laser therapies, the clinical application remains operator-dependent.

Recently, promising results on peri-implantitis were obtained by Namour and collaborators [21] using a new 1064-nm Q-switch Nd:YAG nanosecond pulse. Indeed, effective decontamination with the 1064-nm Nd:YAG laser was observed. However, its effects on implant prosthesis materials such as titanium are not yet fully known.

Therefore, our comparative *in vitro* study aimed to test the effects of 1064-nm Q-switch Nd:YAG nanosecond pulse on titanium surfaces. Plus, the new laser effects were compared with 1064-nm Nd:YAG and 980-nm diode lasers routinely employed for peri-implantitis management through laser therapy [11].

The predictor variable of this study was the peculiar ability of the 1064-nm Q-switch Nd:YAG nanosecond pulse to emit pulses in nanoseconds (ns) and provide a peak power of about 25 kW [21].

The primary variable was to point out the effect of this laser on titanium surfaces.

The secondary object of the investigation was to show the reliability of 1064-nm Q-switch Nd:YAG nanosecond pulse employment compared to the 1064-nm Nd:YAG and 980-nm diode laser. Scanning electron microscopy was used to evaluate the titanium grade 4 surface after laser treatments, and the analysis of roughness change with three-dimensional reconstruction was performed through atomic force microscopy to point out the different effects of irradiations.

2. Materials and Methods

2.1. Study Design

Grade 4 titanium disc samples “FINOFRAME TI-4” (FINO-Gmbh, Mangesfeld 18, 97708 Bad Bocklet, Germany) were used in our study because this is the most commonly used grade of titanium to produce dental implants [22]. The sample was divided into 4 equal slides, as shown in (Figure 1). One slide was not treated and considered as a control (a). Three slides were treated with the lasers 1064-nm Nd:YAG (b), 980-nm diode (c), or 1064-nm Q-switch Nd:YAG nanosecond pulse (d), through the parameters described in Table 1. All of the lasers used were produced by the Italian company DMT Srl. (20851—Via Nobel 1 Lissone (MI)-Italy).

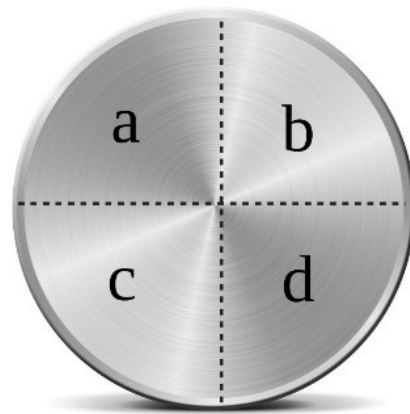


Figure 1. Design of the treated area on a titanium grade 4 disc: (a) no-treated area (control); (b) area treated with 1064 nm Nd-YAG; (c) area treated with 980 nm Diode; (d) area treated with 1064 nm Q-Switch Nd-YAG.

Table 1. Laser specifics and parameters of irradiation. Parameters were chosen according to the therapies for peri-implant disease programs that each company of laser device set.

| LASER | 1064 nm Nd-Yag b | 980 nm Diodo c | 1064 nm Q-Switch Nd-Yag d |
|-------------------------------------|--|---|---|
| WAVELENGTH | 1064-nm | 980-nm | 1064-nm |
| PRIMARY POWER | 10 W | 7 W | 1.5 W |
| POWER PEAK | 3500 W | 15 W | 25 KW |
| FREQUENCY | 200 Hz | 1000 Hz | 500 Hz |
| PULSE DURATION | 50–500 us | 1 ms—CW | 3 ns |
| CLASS MEDICAL EQUIPMENT | IIB | IIB | IIB |
| CLASS OF THE LASER | IV | IV | IV |
| PARAMETERS USED FOR THE STUDY | 1.5 W 50 us pulse 10 Hz 3500 W power peak | 1.5 W gated mode 10 ms Ton 10 ms Toff 320 um fiber | 1.5 W 3 ns pulse 20,000 Hz 25,000 W power peak |

Since the oral environment could influence the effects on peri-implants, a bioreactor simulating the saliva and titanium interaction was designed (Figure 2). The bioreactor was able to mimic the saliva composition, humidity, pH, and temperature characteristics of the oral environment. Essentially, a thermostatic bath with a recirculation pump (Grant model ST 12; Grant Instruments Cambridge, SG8 6GB, Cambridgeshire, United Kingdom) was filled with distilled water to keep the temperature constant and contain a cubic glass tank (15 cm for side) immersed. A stub was then glued to the bottom of the cubic glass tank by a two-component adhesive (Tintoke 3M, Saint Paul, Minnesota, USA) to support the titanium disc. Fifty centilitres of a salivary substitute solution (0.103 g/L of CaCl₂, 0.019 g/L MgCl₂·6H₂O, 0.544 g/L KH₂PO₄, 2.24 g/L KCl, and TCP-KOH buffer, final pH = 7.0) was added [23]. The pH of the artificial saliva was balanced by measuring it with the Five Easy Plus pH Meter FP20-Std-Kit, (Mettler Toledo, Columbus, OH, USA). The thermostatic tank with a recirculation pump was activated to induce a temperature of 37.5 °C, which was measured with the double probe K thermocouple thermometer, HI 935002 digital thermometer, K probe, 2 inputs (HANNA INSTRUMENTS Italia srl—Viale Delle Industrie, 11—35010 Ronchi di Villafranca Padovana, Italy). Additionally, the humidity was maintained at around 93 Kg/m³ and measured with the HI9564 digital thermo-hygrometer (HANNA INSTRUMENTS Italia srl) [24,25].

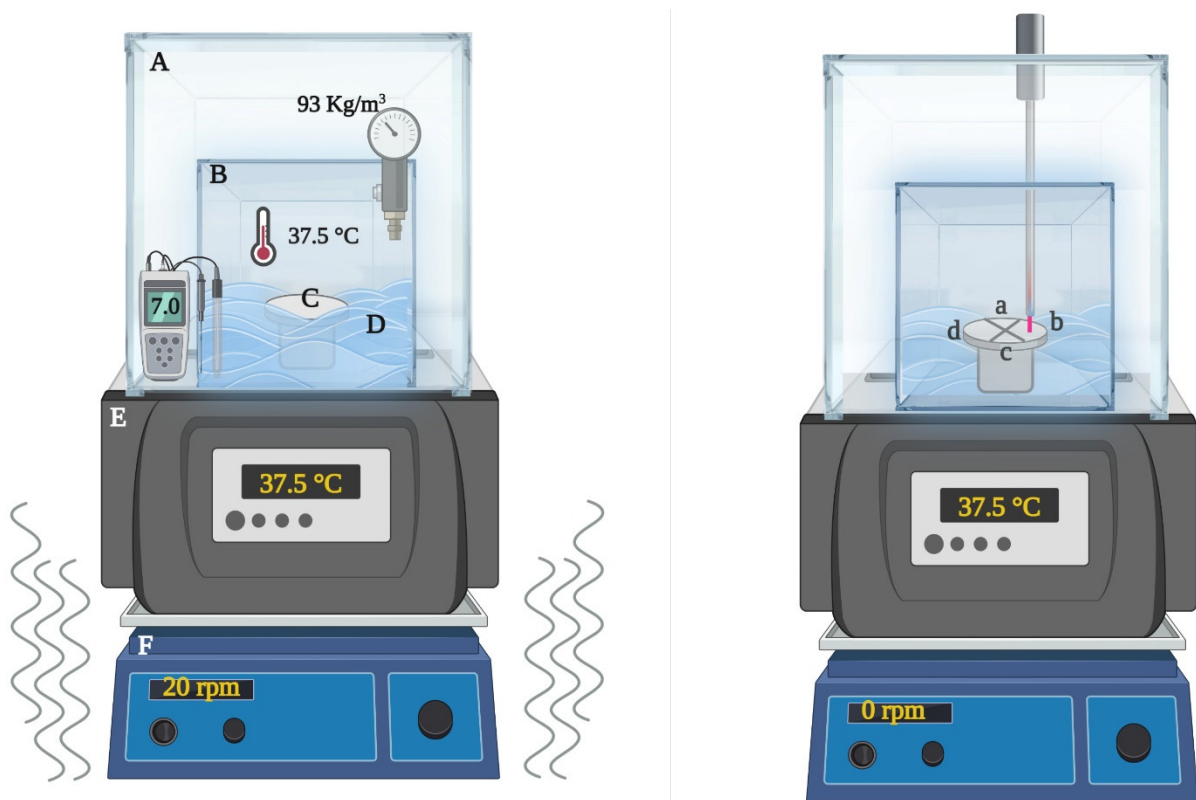


Figure 2. Oral cavity bioreactor simulator. The bioreactor consisted of a thermostatic bath (A) filled with distilled water to keep the temperature constant at 37.5 °C (A,E). The bath contained a cubic glass tank (B) immersed. A stub supported the titanium disc on the tank bottom (C). Salivary substitute solution (D) was kept shaking at 20 rpm (F) to allow the oscillating artificial saliva to touch the titanium surface of the samples (left). The titanium disc was pre-incubated inside the bioreactor for 7 days before the experiments took place. The irradiation was performed at 0 rpm, with an optical fibre able to irradiate the titanium disc slides (b,c,d) according to the parameters described in Table 1 (right). (a) Not-irradiated slide (control). The pH (7.0), temperature (37.5 °C), and humidity (93 kg/m³) were monitored through a pH Meter, a thermocouple, and a digital thermo-hygrometer, respectively.

The structure was placed on the top of an orbital shaker (SLA-OS-200. Scitech LabApp Ltd., Micklefield, Leeds, LS25 9BP, UK) set at 20 rpm to allow the oscillating artificial saliva to touch the titanium surface of the samples. The titanium discs were pre-incubated inside the bioreactor for 7 days before the experiments took place.

According to Namour and collaborators [21], the irradiation was performed with a 320 µm optical fibre provided by the laser device companies for each laser employed. The fibre was fixed to a Laboratory Stand at a distance of 500 µm from the surface of the treated area. The setup allowed for keeping the 50 mm² irradiated surface constant and also avoided reaching parts of the other group.

To mimic the clinical treatments *in vivo*, the irradiations were performed through the parameters described in Table 1 and according to both Świder and collaborators [11] and Namour and collaborators [21].

The precision of the irradiated power was secured by the Pronto-250 power meter (Gentec Electro-Optics, Inc., Quebec, QC, Canada).

During the treatment, the temperature was monitored through an FLIR ONE Pro-iOS professional thermal imaging camera (FLIR Systems, Inc., designs, Portland, OR, USA) (dynamic range: −20 °C/+400 °C; resolution 0.1 °C).

2.2. Scanning Electron Microscope (SEM) Analysis

The irradiated slide samples and the slide control were morphologically evaluated using an SEM Hitachi S-2500, (Hitachi Sefton Park Bells, Hill Stoke Poges, Buckinghamshire, SL2 4HD, UK). It was not necessary to carry out a metallisation of the sample surfaces since titanium presents an electrical conductivity that is useful for SEM analysis.

All images were acquired in secondary electrons at 10 KV with 50× magnification and recorded with a Nikon F50 digital camera.

2.3. Atomic Force Microscopy

In order to obtain quantitative information regarding the surface profile (i.e., surface topography), we employed atomic force microscopy (AFM) to image with high resolution the surface, before and after laser treatments. Every sample was carefully ultrasonicated and cleaned with distilled water and 70% ethanol. Contact mode AFM images were obtained using a Nanowizard JPK Bioafm (Bruker) and a Zeiss optical microscope (Axio Zoom V16) to find and position the AFM probe onto the area of interest. CSG11-A cantilevers (Mikro-Masch), with a nominal spring constant $K = 0.1 \text{ N/m}$, were used for acquisitions. Images were collected in pure water over a $70 \times 70 \mu\text{m}^2$ area at a resolution of 256×256 pixels, a constant deflection of 150 nm, and a scan rate of 0.4 Hz. We selected at least 3 images for each sample for roughness analysis. Data were processed using the Mountains[®] software Premium 9.2.9994 courtesy of Digital Surf, France, and a plane correction process was performed on all the AFM topographical images [26]. The changes in roughness parameters and the surface topography of each sample were investigated before and after the titanium surface interaction with the three lasers used. The selected roughness parameters are the most widespread among relevant amplitude parameters and were calculated following the ISO 25178 standard as reported below [27,28].

Roughness average:

$$Sa = \dots \frac{1}{MN} \sum_{k=0}^{M-1} \sum_{i=0}^{N-1} |z(x_k, y_i)|$$

where $M \times N =$ total number of scan points.

Root mean square:

$$Sq = \sqrt{\frac{1}{MN} \sum_{k=0}^{M-1} \sum_{i=0}^{N-1} [z(x_k, y_k)]^2} \quad (1)$$

Peak-to-peak height: $Sz = z_{max} - z_{min}$, defined as the height difference between the highest and lowest pixel in the image.

The results of the quantitative analysis were expressed as mean value \pm standard error. Statistical analyses were performed using one-way ANOVA plus Tukey's post-test and p -values ≤ 0.01 were regarded as statistically significant.

3. Results

3.1. Analysis of Temperature after Laser Treatments

The detection of any surface temperature increase was carried out during irradiation (Table 2).

Table 2. Increase in temperature during laser-titanium interactions.

| | T0 | T1 | ΔT |
|------------------------------|---------|---------|------------|
| 980 nm Diode | 31.2 °C | 57 °C | 25.8 °C |
| 1064 nm Nd-YAG | 31.2 °C | 55.4 °C | 24.2 °C |
| 1064 nm Q-switch Nd-YAG nano | 31.2 °C | 34.1 °C | 2.9 °C |

From a basic starting point of 31.2 °C, the treatment with the 980 nm diode laser reached 57 °C in two seconds of interaction, thus raising the temperature by 25.8 °C.

Using the 1064-nm Nd-YAG laser, starting from 31.2 °C, it reached 55.4 °C within two seconds of interaction, raising the temperature by 24.2 °C.

Finally, in the two-second interaction with the 1064-nm Q-switch Nd:YAG nanosecond pulse laser, starting from 31.2 °C, we arrived at 34.1 °C with a temperature increase of 2.9 °C.

3.2. Scanning Electron Microscope (SEM) Results

The scanning electron microscope images show the effects caused by the interaction of the different irradiated laser parameters on the grade 4 titanium surface.

Compared to the control image (Figure 3A), the 980 nm diode laser did not seem to negatively affect the grade 4 titanium surface (Figure 3B). However, the regular and compact texture of the control sample changed in apparently more surface roughness due to the exposure of irregular micro-crystallites of the average dimension of about 50 µm. A very small increase in the dimension of the micropores and their irregular shape could also be observed after the treatment with a 980 nm diode laser.

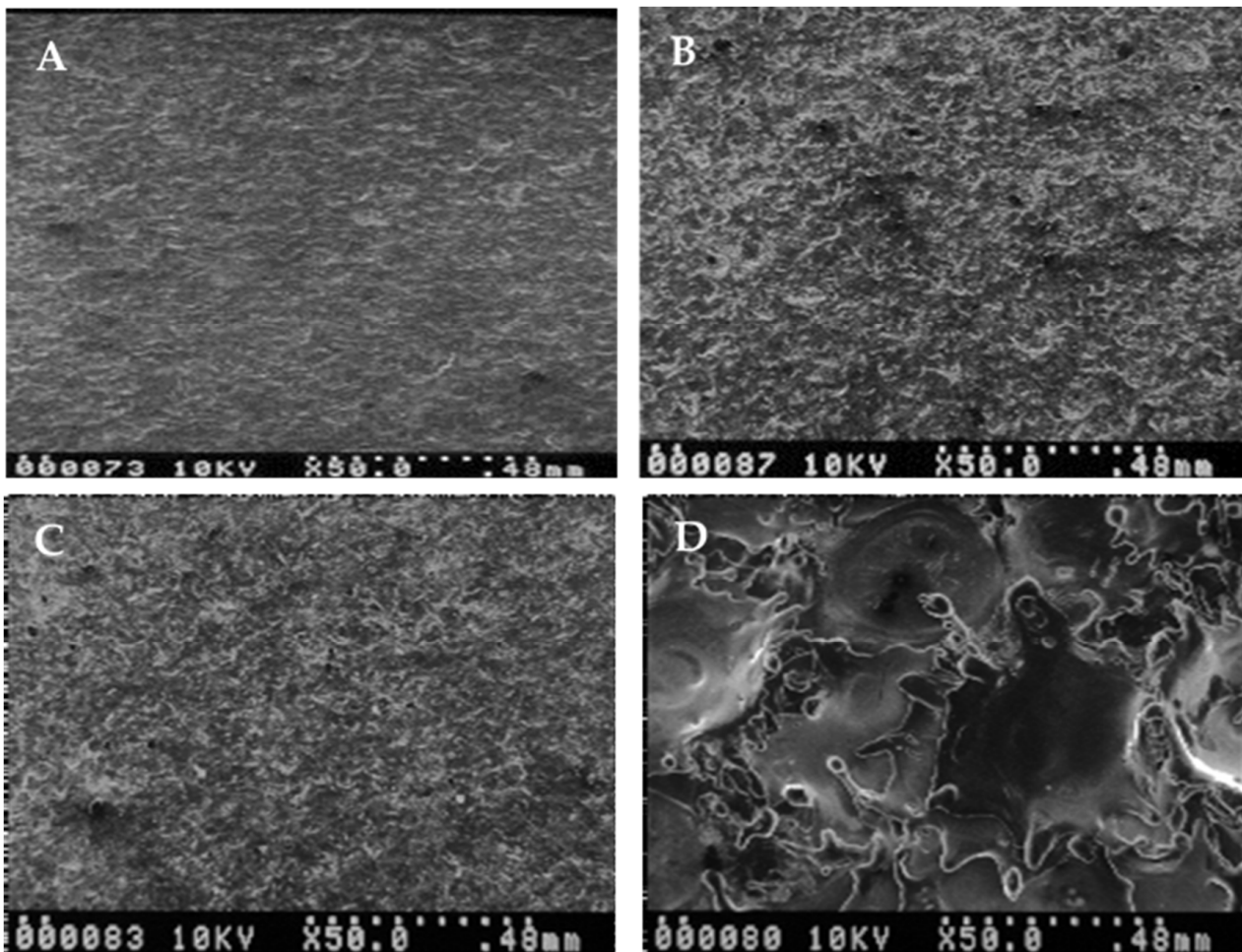


Figure 3. Scanning electron microscope images: (A) = control; (B) = 980 nm diode; (C) = 1064 nm Q-switch Nd-YAG nano; (D): 1064 Nd-YAG.

The same interpretation can be obtained from the image relating to the exposure to the 1064-nm Q-switch Nd:YAG nanosecond pulse laser, which did not seem to notably change the surface morphology of the grade 4 titanium sample examined (Figure 3C), although a moderate alteration of the roughness also occurred in this case.

On the contrary, in the portion of the sample treated with the 1064-nm Nd-YAG laser, significant morphological alterations can be seen. Indeed, melting-like effects on the metal surfaces are visible, which can reach deformations in the range of 3 mm (Figure 3D). Rounded and overlapped plates of about 0.5 mm in diameter with very irregular boundaries but with a smooth cup-shape covered all of the surfaces analysed.

3.3. Atomic Force Microscopy Results

Figure 4 shows representative 3D AFM topography images of the control region and the three treated regions. AFM topography imaged ($70 \mu\text{m} \times 70 \mu\text{m}$) of the control region and the three treated regions after a plane fitting procedure to compensate for sample tilt.

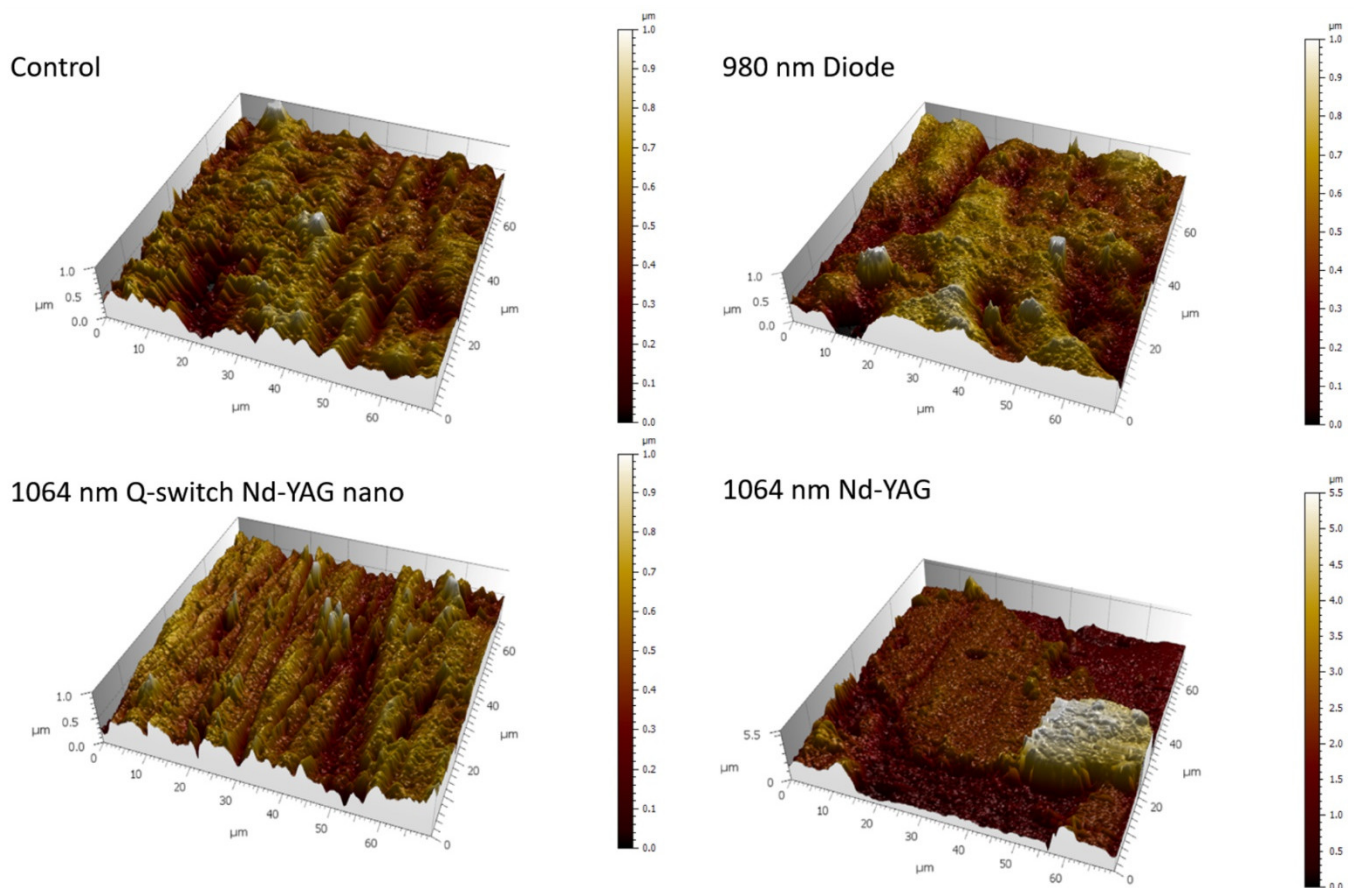


Figure 4. The 3D atomic force microscopy topography images ($70 \times 70 \mu\text{m}$) of the control region and the three treated regions after a plain fitting procedure to compensate for the simple tilt.

Figure 5 shows the height distribution graphs calculated for each image shown in Figure 4. The height differences, calculated as the width of the graphs corresponding to 90% of the distribution (distance between cursors c1 and c2), are reported in the following Table 3 and Figure 5.

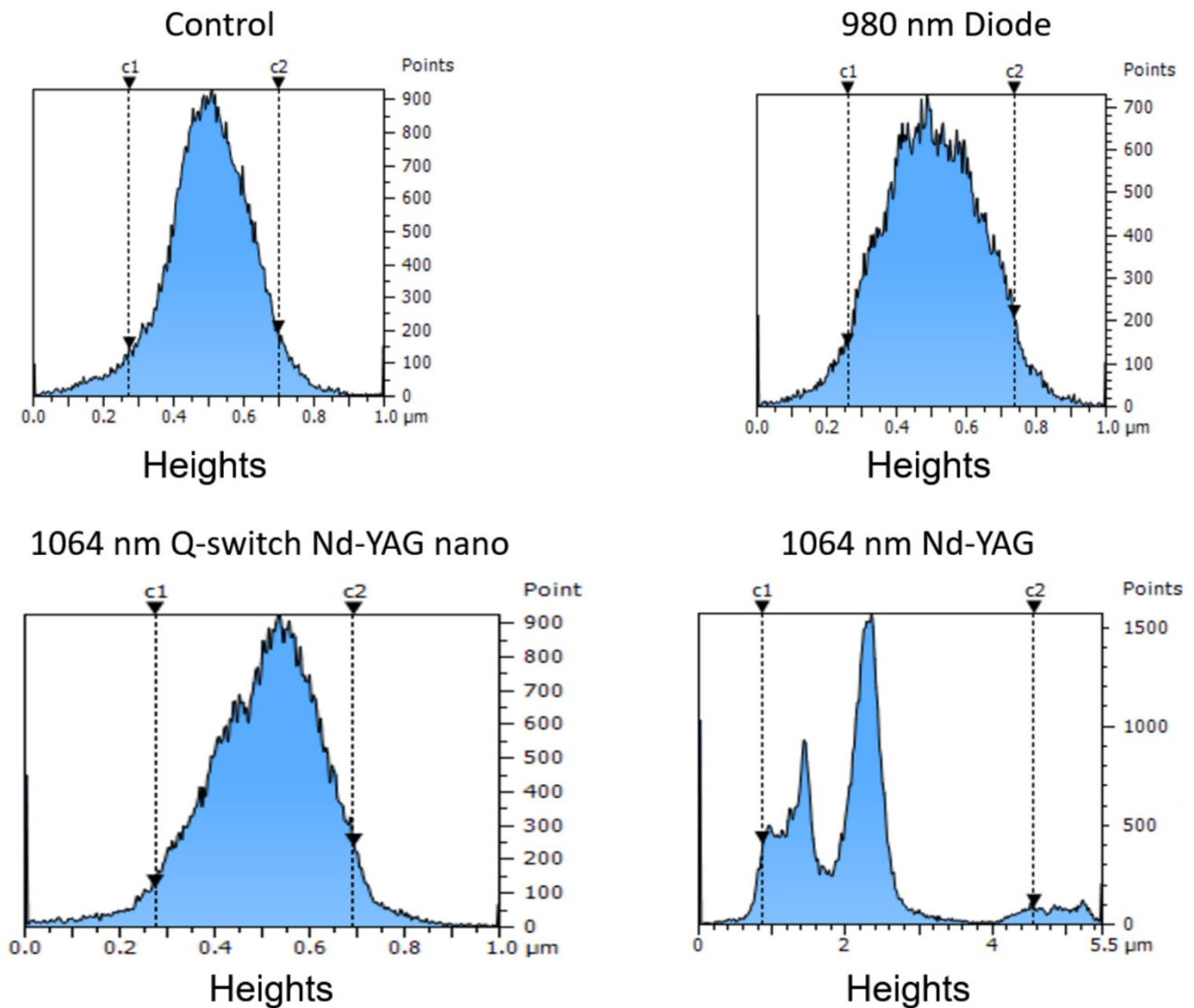


Figure 5. Height distribution histograms of the four images reported in Figure 3. c1 and c2 define the regions corresponding to 90% of the height values.

Table 3. The width of 90% of the height distributions for each image is reported in Figure 4.

| Sample | Height Difference (c1–c2) [μm] |
|------------------------------|---|
| Control Ti | 0.4246 |
| 980 nm Diode | 0.4771 |
| 1064 nm Q-switch Nd-YAG nano | 0.4184 |
| 1064 nm Nd-YAG | 3.7050 |

In order to quantify surface roughness, we calculated three different parameters for each sampled region, namely average roughness Sa , root mean square Sq , and peak-to-peak height Sz . Table 4 and Figure 6 report average roughness values and standard errors for each region.

Table 4. Roughness parameters from the surface analysis of AFM topography images. Average and standard error values were calculated over *n* images.

| Sample | Roughness Parameters | | | |
|------------------------------|----------------------|----------------------|----------------------|----------|
| | Sa [μm] | Sq [μm] | Sz [μm] | <i>n</i> |
| Control Ti | 0.109 \pm 0.007 | 0.147 \pm 0.013 | 2.470 \pm 0.538 | 4 |
| 980 nm diode | 0.140 \pm 0.036 | 0.174 \pm 0.041 | 1.824 \pm 0.300 | 5 |
| 1064 nm Q-switch Nd-YAG nano | 0.150 \pm 0.002 | 0.157 \pm 0.006 | 4.842 \pm 0.605 | 6 |
| 1064 nm Nd-YAG | 0.868 \pm 0.550 | 1.189 \pm 0.651 | 9.278 \pm 3.010 | 3 |

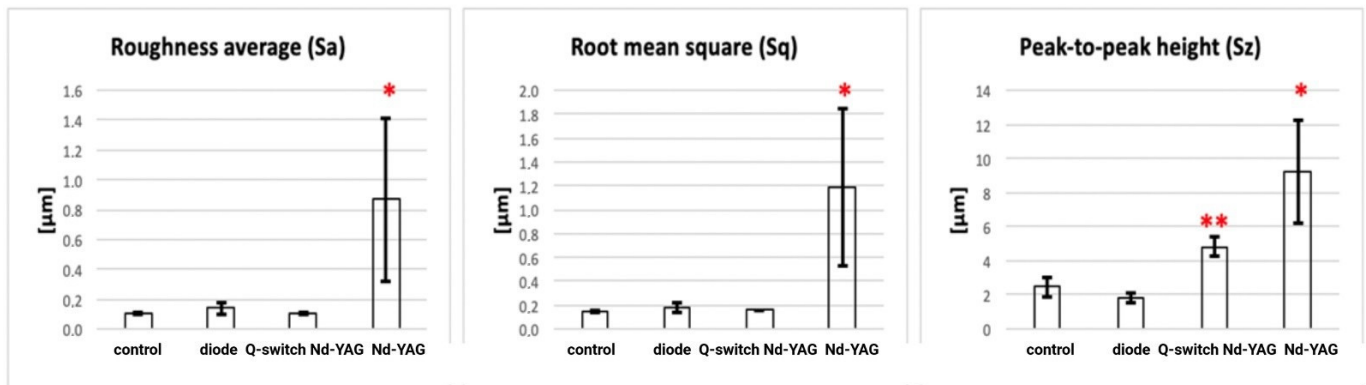


Figure 6. Roughness parameter values were calculated from the surface analysis of AFM topography images. * and ** $p \leq 0.01$ indicate statistically significant differences.

4. Discussion

The main aim of this work was to test the effects of the 1064-nm Q-switch Nd:YAG nanosecond pulse on titanium surfaces, compared to the 1064-nm Nd:YAG and 980-nm diode lasers routinely employed for peri-implant infection management.

Given the great growth in the use of different laser wavelengths for the treatment of periodontal and peri-implant disease [21], it was important to carry out an investigation. The focus of our study was to highlight possible harmful behaviours dictated by the interaction of these devices with the materials used for the dental implant. From the data collected from our experiments, significant differences can be seen based on the type of laser interacting with the grade 4 titanium sample. Observation of the sample under the scanning electron microscope showed us a damaged surface when it interacted with 1064-nm Nd:YAG, where the conspicuous morphological changes comparable to craters [29] constituted sections that are colonisable by bacterial species that are capable of worsening the peri-implant health conditions of the host [21,30]. On the other hand, the images relating to the sample interacting with a 980nm diode laser and 1064-nm Q-switch Nd:YAG nanosecond pulse laser showed no signs of damage to the morphology of the grade 4 titanium surface, but only a slight modification of the surface. This is due to the removal of the more external coating and as a consequence of the exposure to the micro-crystallites of titanium and of some micropores that induce a very slight increase in roughness, as confirmed by the AFM results.

From the roughness parameter evaluation, the results showed a small increase in Sa values for 1064-nm Q-switch Nd:YAG nanosecond pulse and 980-nm diode-treated parts, with respect to control values, but this is quite negligible when compared to the 1064-nm Nd:YAG treated one. This can indicate that the average absolute deviations of the roughness irregularities are comparable for these considered surfaces, while the treatment with 1064-nm Nd:YAG generated greater defects on the titanium surface. These considerations can be confirmed by the values of the Sq parameter, which is even more sensitive to surface deviations, and can be considered a reliable complementary parameter.

The height distribution histograms also showed a greater height difference for the 1064-nm Nd:YAG-treated surface when compared to the other regions, as specified in Figure 6. The height axis of the histograms highlighted the higher and more spread surface irregularities for the 1064-nm Nd:YAG-treated surface, with histograms showing the presence of different peaks within the considered region c1–c2.

For a deeper evaluation, the Sz parameter was calculated since it is more sensitive to randomly distributed peaks or valleys. Both Nd:Yag-treated regions showed higher Sz values when compared to the region treated with the 980-nm diode and the control; nevertheless, if one compares 1064-nm Nd:YAG-treated areas with 1064-nm Q-switch Nd:YAG nanosecond pulse-treated ones, the former would always show significantly higher Sz values.

In conclusion, the results obtained from the roughness analysis suggest that 1064-nm Nd:YAG treatment can be considered the most invasive, while both the 1064-nm Q-switch Nd:YAG nanosecond pulse and 980-nm diode do not significantly affect surface topography. Our 1064-nm Nd:YAG effects meet well with recent work on the erbium-doped yttrium aluminum garnet laser (Er: YAG) at 4 W and 400 mJ/pulse, which induced melting, microcracks, signs of coagulation, and microfractures on grade-4 titanium [31]. Conversely, the Er: YAG at 1 W and 100 mJ/pulse affected the titanium surface, which decreased its porosity and micro-roughness; both represent a positive alteration in terms of prevention of bacterial adhesion [31].

Lastly, considering that the defined thermic rise begins at 5 °C [17] for biological tissue, such as the bone around implants during the osseointegration, we observed that only the 1064-nm Q-switch Nd:YAG nanosecond pulse laser was able to perform its action, without increasing the temperature of the metal beyond that threshold. The 980 nm diode lasers and 1064 nm Nd:YAG instead created a very high-temperature difference and were not compatible with the health of the bone cells around the implant.

5. Conclusions

According to our primary and secondary variables, our data clearly showed that the irradiation device mode and the parameters administered affected the titanium grade 4 surface in different ways. The 1064-nm Q-switch Nd:YAG nanosecond pulse appears to be more suitable for the preservation of implant morphology because of the lack of evidence of the induction of metal damage and, as shown by Namour et al. [21], the efficacy of bacteria decontamination.

The roughness analysis carried out on the acquired AFM topography images revealed the more invasive nature of the 1064-nm Nd:YAG treatment on the sampled titanium surface when compared to the other lasers considered. On the contrary, from this analysis, the difference between 1064-nm Q-switch Nd:YAG nanosecond pulse and 980-nm diode treatments was not significantly different.

Therefore, in order to confirm the effectiveness of the new 1064-nm Q-switch Nd:YAG nanosecond pulse treatment, in terms of the absence of relevant surface alterations, a deeper comparative study between the 1064-nm Q-switch Nd:YAG nanosecond pulse and 980-nm diode should be carried out.

Author Contributions: Conceptualization, C.P., S.B., F.B., A.L. and A.A.; methodology, A.A., F.B. and A.L.; validation, A.A., F.B., R.R. and A.L.; formal analysis, C.P. and E.D.; investigation, C.P. and E.D.; resources, C.P. and S.B.; data curation, C.P., F.B., A.L., E.D., R.R. and A.A.; writing—original draft preparation, C.P. and E.D.; writing—review and editing, F.B., A.L., N.D.A., R.R. and A.A.; supervision, A.A. and R.R. All authors have read and agreed to the published version of the manuscript.

Funding: This research received no external funding.

Institutional Review Board Statement: Not applicable.

Informed Consent Statement: Not applicable.

Data Availability Statement: Data available on request from the authors.

Conflicts of Interest: The authors declare no conflict of interest.

References

- Pranno, N.; la Monaca, G.; Polimeni, A.; Sarto, M.S.; Uccelletti, D.; Bruni, E.; Cristalli, M.P.; Cavallini, D.; Voza, I. Antibacterial Activity against Staphylococcus Aureus of Titanium Surfaces Coated with Graphene Nanoplatelets to Prevent Peri-Implant Diseases. An In-Vitro Pilot Study. *Int. J. Environ. Res. Public Health* **2020**, *17*, 1568. [[CrossRef](#)] [[PubMed](#)]
- Klinge, B.; Lundström, M.; Rosén, M.; Bertl, K.; Klinge, A.; Stavropoulos, A. Dental Implant Quality Register—A Possible Tool to Further Improve Implant Treatment and Outcome. *Clin. Oral Implants Res.* **2018**, *29*, 145–151. [[CrossRef](#)] [[PubMed](#)]
- Berglundh, T.; Armitage, G.; Araujo, M.G.; Avila-Ortiz, G.; Blanco, J.; Camargo, P.M.; Chen, S.; Cochran, D.; Derks, J.; Figuero, E. Peri-Implant Diseases and Conditions: Consensus Report of Workgroup 4 of the 2017 World Workshop on the Classification of Periodontal and Peri-Implant Diseases and Conditions. *J. Clin. Periodontol.* **2018**, *45*, 286–291. [[CrossRef](#)] [[PubMed](#)]
- Najeeb, S.; Zafar, M.S.; Khurshid, Z.; Zohaib, S.; Almas, K. The Role of Nutrition in Periodontal Health: An Update. *Nutrients* **2016**, *8*, 530. [[CrossRef](#)] [[PubMed](#)]
- Niazi, F.; Naseem, M.; Khurshid, Z.; Zafar, M.S.; Almas, K. Role of Salvadora Persica Chewing Stick (Miswak): A Natural Toothbrush for Holistic Oral Health. *Eur. J. Dent.* **2016**, *10*, 301.
- Matsuda, S.; Movila, A.; Suzuki, M.; Kajiyama, M.; Wisitrasameewong, W.; Kayal, R.; Hirshfeld, J.; Al-dharrab, A.; Savitri, I.J.; Mira, A. A Novel Method of Sampling Gingival Crevicular Fluid from a Mouse Model of Periodontitis. *J. Immunol. Methods* **2016**, *438*, 21–25. [[CrossRef](#)]
- Mombelli, A.; Décaillet, F. The Characteristics of Biofilms in Peri-Implant Disease. *J. Clin. Periodontol.* **2011**, *38*, 203–213. [[CrossRef](#)]
- Mombelli, A.; van Oosten, M.A.C.; Schürch, E.; Lang, N.P. The Microbiota Associated with Successful or Failing Osseointegrated Titanium Implants. *Oral Microbiol. Immunol.* **1987**, *2*, 145–151. [[CrossRef](#)]
- Hanna, R.; Dalvi, S.; Benedicenti, S.; Amaroli, A.; Sălăgean, T.; Pop, I.D.; Todea, D.; Bordea, I.R. Photobiomodulation Therapy in Oral Mucositis and Potentially Malignant Oral Lesions: A Therapy Towards the Future. *Cancers* **2020**, *12*, 1949. [[CrossRef](#)]
- Lin, G.H.; Suárez López Del Amo, F.; Wang, H.L. Laser Therapy for Treatment of Peri-Implant Mucositis and Peri-Implantitis: An American Academy of Periodontology Best Evidence Review. *J. Periodontol.* **2018**, *89*, 766–782.
- Świder, K.; Dominiak, M.; Grzech-Leśniak, K.; Matys, J. Effect of Different Laser Wavelengths on Periodontopathogens in Peri-Implantitis: A Review of In Vivo Studies. *Microorganisms* **2019**, *7*, 189. [[CrossRef](#)]
- Albaker, A.M.; ArRejaie, A.S.; Alrabiah, M.; Abduljabbar, T. Effect of Photodynamic and Laser Therapy in the Treatment of Peri-Implant Mucositis: A Systematic Review. *Photodiagn. Photodyn. Ther.* **2018**, *21*, 147–152. [[CrossRef](#)]
- Pontoriero, R.; Tonelli, M.P.; Carnevale, G.; Mombelli, A.; Nyman, S.R.; Lang, N.P. Experimentally Induced Peri-Implant Mucositis. A Clinical Study in Humans. *Clin. Oral Implants Res.* **1994**, *5*, 254–259. [[CrossRef](#)]
- Rösing, C.K.; Fiorini, T.; Haas, A.N.; Muniz, F.W.M.G.; Oppermann, R.V.; Susin, C. The Impact of Maintenance on Peri-Implant Health. *Braz Oral Res.* **2019**, *33*, e074. [[CrossRef](#)]
- Esposito, M.; Worthington, H.V.; Thomsen, P.; Coulthard, P. Interventions for Replacing Missing Teeth: Maintaining Health around Dental Implants. *Cochrane Database Syst. Rev.* **2004**, *3*, CD003069.
- Amaroli, A.; Colombo, E.; Zekiy, A.; Aicardi, S.; Benedicenti, S.; de Angelis, N. Interaction between Laser Light and Osteoblasts: Photobiomodulation as a Trend in the Management of Socket Bone Preservation—A Review. *Biology* **2020**, *9*, 409. [[CrossRef](#)]
- Pasquale, C.; Colombo, E.; Benedicenti, S.; Signore, A.; Amaroli, A.; Pasquale, C.; Colombo, E.; Benedicenti, S.; Signore, A.; Amaroli, A. 808-Nm Near-Infrared Laser Photobiomodulation versus Switched-Off Laser Placebo in Major Aphthae Management: A Randomized Double-Blind Controlled Trial. *Appl. Sci.* **2021**, *11*, 4717. [[CrossRef](#)]
- Roncati, M.; Lucchese, A.; Carinci, F. Non-Surgical Treatment of Peri-Implantitis with the Adjunctive Use of an 810-Nm Diode Laser. *J. Indian Soc. Periodontol.* **2013**, *17*, 812–815.
- Oyster, D.K.; Parker, W.B.; Gher, M.E. CO₂ Lasers and Temperature Changes of Titanium Implants. *J. Periodontol.* **1995**, *66*, 1017–1024. [[CrossRef](#)]
- Basso, F.G.; Oliveira, C.F.; Fontana, A.; Kurachi, C.; Bagnato, V.S.; Spolidório, D.M.P.; Hebling, J.; de Souza Costa, C.A. In Vitro Effect of Low-Level Laser Therapy on Typical Oral Microbial Biofilms. *Braz Dent. J.* **2011**, *22*, 502–510. [[CrossRef](#)]
- Namour, M.; El Mobadder, M.; Magnin, D.; Peremans, A.; Verspecht, T.; Teughels, W.; Lamard, L.; Nammour, S.; Rompen, E. Q-Switch Nd:YAG Laser-Assisted Decontamination of Implant Surface. *Dent. J.* **2019**, *7*, 99. [[CrossRef](#)]
- W.Nicholson, J. Titanium alloys for dental implants: A review. *Prosthesis* **2020**, *2*, 11.
- Sri, A.; Amal, S.; Hussain, S.; Amin Jalaluddin, M. Preparation of Artificial Saliva Formulation. In Proceedings of the International Conference ICB Pharma II, Solo, Indonesia, 31 October 2015.
- Sund-Levander, M.; Forsberg, C.; Wahren, L.K. Normal Oral, Rectal, Tympanic and Axillary Body Temperature in Adult Men and Women: A Systematic Literature Review. *Scand. J. Caring Sci.* **2002**, *16*, 122–128. [[CrossRef](#)] [[PubMed](#)]
- Dabbagh, S.; Hardan, L.; Kassis, C.; Bourgi, R.; Devoto, W.; Zarow, M.; Jakubowicz, N.; Ghaleb, M.; Kharouf, N.; Dabbagh, M. Effect of Intraoral Humidity on Dentin Bond Strength of Two Universal Adhesives: An In Vitro Preliminary Study. *Coatings* **2022**, *12*, 712. [[CrossRef](#)]
- Bonyár, A. AFM Characterization of the Shape of Surface Structures with Localization Factor. *Micron* **2016**, *87*, 1–9. [[CrossRef](#)]

27. Raposo, M.; Ferreira, Q.; Ribeiro, P.A. A Guide for Atomic Force Microscopy Analysis of Soft-Condensed Matter. *Mod. Res. Educ. Top. Microsc.* **2007**, *1*, 758–769.
28. Gadelmawla, E.S.; Koura, M.M.; Maksoud, T.M.A.; Elewa, I.M.; Soliman, H.H. Roughness Parameters. *J. Mater. Process. Technol.* **2002**, *123*, 133–145. [[CrossRef](#)]
29. Romanos, G.E.; Everts, H.; Nentwig, G.H. Effects of Diode and Nd:YAG Laser Irradiation on Titanium Discs: A Scanning Electron Microscope Examination. *J. Periodontol.* **2000**, *71*, 810–815. [[CrossRef](#)]
30. Renvert, S.; Persson, G.R.; Pirih, F.Q.; Camargo, P.M. Peri-implant health, peri-implant mucositis, and peri-implantitis: Case definitions and diagnostic considerations. *J. Clin. Periodontol.* **2018**, *45*, 278–285. [[CrossRef](#)]
31. Kniha, K.; Heussen, N.; Weber, E.; Möhlhenrich, S.C.; Hölzle, F.; Modabber, A. Temperature Threshold Values of Bone Necrosis for Thermo-Explantation of Dental Implants—A Systematic Review on Preclinical In Vivo Research. *Materials* **2020**, *13*, 3461. [[CrossRef](#)]

Disclaimer/Publisher’s Note: The statements, opinions and data contained in all publications are solely those of the individual author(s) and contributor(s) and not of MDPI and/or the editor(s). MDPI and/or the editor(s) disclaim responsibility for any injury to people or property resulting from any ideas, methods, instructions or products referred to in the content.